Biochemical and Biophysical Research Communications 430 (2013) 1169–1174

Contents lists available at SciVerse ScienceDirect

Biochemical and Biophysical Research Communications

journal homepage: www.elsevier.com/locate/ybbrc

Direct molecular interaction of caveolin-3 with KCa1.1 channel in living HEK293 cell expression system

Yoshiaki Suzuki [a], Hisao Yamamura [a], Susumu Ohya [a,b], Yuji Imaizumi [a,*]

[a] Department of Molecular & Cellular Pharmacology, Graduate School of Pharmaceutical Sciences, Nagoya City University, Nagoya, Japan
[b] Department of Pharmacology, Kyoto Pharmaceutical University, Kyoto, Japan

ARTICLE INFO

Article history:
Received 19 November 2012
Available online 10 December 2012

Keywords:
Caveolin-3
Caveolin-1
BK_{Ca} channel
TIRF
FRET

ABSTRACT

Caveolin family is supposed to be essential molecules for the formation of not only caveola structure on cell membrane but also functional molecular complexes in them with direct and/or indirect interaction with other membrane and/or submembrane associated proteins. The direct coupling of caveolin-1 (cav1) with large conductance Ca^{2+}-activated K^+ channel, KCa1.1 has been established in several types of cells and in expression system as well. The possible interaction of caveolin-3 (cav3), which shows expression in some differential tissues from cav1, with KCa1.1 remains to be determined. In the present study, the density of KCa1.1 current expressed in HEK293 cells was significantly reduced by the co-expression of cav3, as well as cav1. The co-localization and direct interaction of GFP- or CFP-labeled cav3 (GFP/CFP-cav3) with YFP- or mCherry-labeled KCa1.1 (KCa1.1-YFP/mCherry) were clearly demonstrated by single molecular image analyses using total internal reflection fluorescence (TIRF) microscopy and fluorescence resonance energy transfer (FRET) analyses with acceptor photobleaching method. The deletion of suggested cav1-binding motif in C terminus region of KCa1.1 (KCa1.1ΔCB-YFP) resulted in the marked decrease in cell surface expression, co-localization and FRET efficiency with CFP-cav3 and CFP-cav1. The FLAG-KCa1.1 co-immunoprecipitation with GFP-cav3 or GFP-cav1 also supported their direct molecular interaction. These results strongly suggest that cav3 possesses direct interaction with KCa1.1, presumably at the same domain for cav1 binding. This interaction regulates KCa1.1 expression to cell surface and the formation of functional molecular complex in caveolae in living cells.

1. Introduction

The large-conductance Ca^{2+}-activated K^+ (KCa1.1 or BK_{Ca}) channels are ubiquitously expressed in plasma membrane of excitable cells, such as neurons and smooth muscles, except for cardiac myocytes. BK_{Ca} channel is activated by both membrane depolarization and elevated cytosolic Ca^{2+} [1]. The major role of BK_{Ca} channels is considered to be the contribution to the negative feedback mechanism in cellular Ca^{2+} regulation by reducing membrane excitability and/or voltage-gated Ca^{2+} channel activities via Ca^{2+}-dependent membrane hyperpolarization [2]. In mammalian skeletal muscle cells, BK_{Ca} channels are localized at T-tubules and sarcolemma [3,4]. It has been found that, in *Caenorhabditis elegans*, BK_{Ca} channel regulates Ca^{2+} transients and maintains muscle excitability in body-wall muscle cells and controls neurotransmitter release in presynaptic nerve terminal [5]. Several auxiliary subunits of BK_{Ca} channel [6,7], a cytoskeletal protein [8,9] and molecular complex with dystrophin [5,10,11], which provide a link between the cytoskeleton and the extracellular matrix, are required for proper BK_{Ca} channel subcellular localization and functional activities in skeletal muscle.

Caveolae are Ω-shaped invaginations on the membrane surface (50–100 nm in diameter) that contain caveolin proteins and form cellular signal domain but can also function as carriers in the exocytic and endocytic pathways [12–14]. Among three caveolin members, caveolin-1 (cav1) is abundant in caveolae-rich non-muscle cells and smooth muscle cells and occasionally forms hetero-oligomers with caveolin-2 (cav2). In contrast, caveolin-3 (cav3) is abundantly expressed in striated muscles and also found in some smooth muscle cells. Cav-3 is transiently associated with T-tubule system during early development to myotubes, whereas in mature myocytes it is localized to caveolae of plasma membrane (sarcolemma) and the necks of T-tubules [15]. Within the sarcolemma, cav3 belongs to the dystrophin complex and is essential to confer stability to sarcolemma. Several specific cav3 mutants and loss of cav3 lead to skeletal muscular disease, such as limb gridle muscular dystrophy (LGMD-1C), hyper CKemia, rippling muscle disease and distal myopathy [15].

It has been well established that BK_{Ca} channel interacts with cav1 [16–18]. In the previous study, we have shown the direct and functional interaction of BK_{Ca} channel with cav1 to form

* Corresponding author. Address: Department of Molecular & Cellular Pharmacology, Graduate School of Pharmaceutical Sciences, Nagoya City University, 3-1 Tanabedori, Mizuho-ku, Nagoya 467-8603, Japan. Fax: +81 52 836 3431.
E-mail address: yimaizum@phar.nagoya-cu.ac.jp (Y. Imaizumi).

0006-291X/$ - see front matter © 2012 Elsevier Inc. All rights reserved.
http://dx.doi.org/10.1016/j.bbrc.2012.12.015

functional molecular complex in living vascular smooth muscle cells and also in HEK293 expression system [19]. It remains, however, to be determined whether BK_{Ca} channel directly interacts with cav3, whereas the possible functional interaction between BK_{Ca} channel and dystrophin complex including cav3 in skeletal muscle has been suggested [5,11].

The present study was undertaken to examine the possible molecular interaction between BK_{Ca} channel α-subunit (KCa1.1 or KCNMA1) and cav3 in HEK cell expression system using single molecular imaging with TIRF microscopy. The advantages of the methods are as follows: (i) Molecular interaction can be detected from living cells under the simultaneous measurements of molecular functions by patch-clamp. (ii) The ratio of coupling and uncoupling molecules can be detected by trajectory analyses of co-localized fluorescent signals for over a minute and also by FRET analyses in living cells [19].

2. Methods

2.1. Cell culture

HEK293 cell line was obtained from the Health Science Research Resources Bank (Osaka, Japan) and cultured in Dulbecco's Modified Eagle's Medium supplemented with 10% heat-inactivated fetal bovine serum, 20 U/ml penicillin, and 20 μg/ml streptomycin (Sigma–Aldrich, St. Louis, MO, USA) at 37 °C.

2.2. Plasmid constructs and transfection

The full-length of cDNA encoding the human KCNMA1 (BKα) subunit (NM_002247) was subcloned into pEYFP-N1 (KCa1.1-YFP) and pmCherry-N1 (KCa1.1-mCherry) (Clontech Laboratories, Mountain View, CA, USA). The KCa1.1-ΔCB construct was generated by PCR and subcloned into pEYFP-N1 (KCa1.1ΔCB-YFP). Human CAV1 (NM_001753) and CAV3 (NM_001234) were also subcloned into pECFP-C1 (CFP-cav1 and CFP-cav3) and pAcGFP1-C1 (GFP-cav1 and GFP-cav3). All constructs were confirmed by DNA sequencing. HEK293 cells were transiently transfected with fluorescent-labeled cDNA (1 μg of KCNMA1 and 0.5 μg of CAV1 or CAV3 cDNA) using LipofectAMINE 2000 (Invitrogen, Carlsbad, CA, USA). Experiments were preformed 48–72 h after transfection.

2.3. TIRF imaging

Single-molecule imaging was performed using the TIRF imaging system (Nikon, Tokyo, Japan) equipped with a fluorescent microscope (ECLIPSE TE2000-U; Nikon), an objective lens (CFI Apo TIRF 100×/1.49, oil immersion; Nikon), an EM-CCD camera (C9100-12; Hamamatsu Photonics, Hamamatsu, Japan), and an AQUACOSMOS software (version 2.6; Hamamatsu Photonics) [19]. GFP- or mCherry-fused protein was excited with a 488-nm argon laser or 543-nm He/Ne laser (Coherent, Santa Clara, CA, USA), respectively. GFP/mCherry emissions were collected through dichroic mirrors and dual band-pass filters (505–530/570–660 nm; Omega Optical, Brattleboro, VT, USA). The resolution of images was 107 nm per pixel ($x - y$) and less than 200 nm (z). TIRF images were collected at 243 ms exposure time and scanned every 1 s. The recording solution had an ionic composition (mM) of 137 NaCl, 5.9 KCl, 2.2 $CaCl_2$, 1.2 $MgCl_2$, 14 glucose, and 10 HEPES. The pH was adjusted to 7.4 with 10 N NaOH. All experiments were carried out at room temperature (25 °C).

2.4. FRET analysis

FRET efficiency (E_{FRET}) was evaluated based on the acceptor photobleaching method, in which the emission of the donor fluorophore is compared before and after photobleaching of the acceptor [19]. The fluorescence of YFP was photobleached using a mercury lamp (100 W, C-SHG1; Nikon) and a G-2A filter cube (Ex510–560/DM575/BA590; Nikon) for 1.5 min. Ten images using 405 and 488 laser lines were acquired at 20 Hz before and after photobleaching of YFP fluorophores. For TIRF/FRET analysis, emissions of CFP and YFP were collected using CFP-HQ (DM450/BA460-510; Nikon) and YFP-HQ (DM510/BA520-560; Nikon) filter cubes, respectively. E_{FRET} was calculated as the percentage increase in CFP emission after YFP photobleaching using the following equation: E_{FRET} (%) = $((CFP_{after} - CFP_{before})/CFP_{after}) \times 100$, where CFP_{after} and CFP_{before} are CFP emissions after and before YFP photobleaching, respectively. Fluorescence intensity was calculated by drawing a region within the cell and subtracting the background in a cell-free region.

2.5. Electrophysiological recording

Electrophysiological studies were performed using a whole cell voltage clamp technique with a CEZ-2400 amplifier (Nihon Kohden, Tokyo, Japan), an analog–digital converter (DIGIDATA 1440A; Axon Instruments, Foster City, CA, USA) and pCLAMP software (version 10.3; Axon Instruments). For BK_{Ca} channel current measurements, the pipette solution contained (mM) 140 KCl, 2.8 $MgCl_2$, 10 HEPES, 2 Na_2ATP, 5 EGTA and 4.24 $CaCl_2$ (pCa 6.0). The pH was adjusted to 7.2 with KOH. The extracellular solution had an ionic composition (mM) of 137 NaCl, 5.9 KCl, 2.2 $CaCl_2$, 1.2 $MgCl_2$, 14 glucose, and 10 HEPES. The pH was adjusted to 7.4 with NaOH. Whole cell BK_{Ca} channel currents were activated from a holding potential of −80 mV by applying 150-ms voltage steps, once every 10 s, to a voltage range between −60 and 120 mV in increments of 20 mV. BK_{Ca} channel component was determined as 1 μM paxilline sensitive current.

2.6. Drugs

The source of pharmacological agents were as follows: EGTA and HEPES (Dojin, Kumamoto, Japan), paxilline (Tocris Bioscience, Bristol, UK).

2.7. Statistics

Pooled data are shown as the mean ± SE. Statistical significance between two groups was determined by Student's t-test. Statistical significance among groups was evaluated by Tukey's test. Significant difference is expressed in the figures as $^{*}p < 0.05$ or $^{**}p < 0.01$.

3. Results and discussion

3.1. Caveolin-3 attenuated BK_{Ca} channel currents

Here, we examined effects of co-expression of cav3 on functional expression of BK_{Ca} channels in HEK293 cells using whole cell patch-clamp recording. HEK293 cells were transiently transfected with cDNAs encoding BK_{Ca} channel labeled with mCherry at its C terminus (KCa1.1-mCherry) and cav3 or cav1 labeled with GFP at N terminus (GFP-cav3 or GFP-cav1). GFP vector was used as a mock control. BK_{Ca} channel currents were recorded using pipette solution containing 1 μM Ca^{2+} and determined as the current component reduced by addition of 1 μM paxilline (Pax), a specific BK_{Ca} channel blocker (Fig. 1A). BK_{Ca} current density at 120 mV in HEK293 cells expressing KCa1.1-mCherry/GFP-cav3 (cav3, 172 ± 51 pA/pF, $n = 5$) was significantly smaller than that in control cells expressing KCa1.1-mCherry/GFP ($p < 0.05$ vs. control; Fig. 1B and C). BK_{Ca} current density in KCa1.1-mCherry/GFP-cav1 (cav1, 77 ± 23 pA/pF, $n = 5$) was also significantly lower than that in

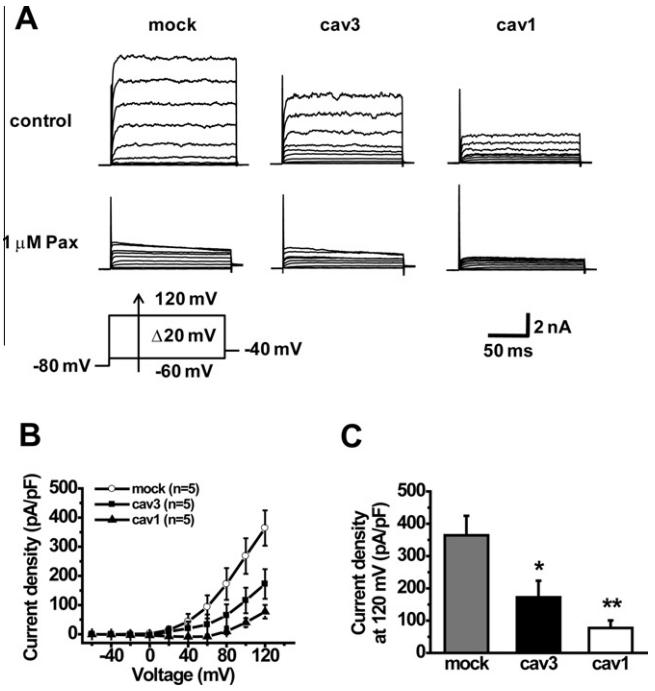

Fig. 1. (A) Representative BK_{Ca} channel currents in GFP-transfected (mock), GFP-cav3-transfected (cav3) or GFP-cav1-trasnsfected (cav1) cells are shown. BK_{Ca} channel component was determined as a current component reduced by addition of 1 μM Pax, a specific BK_{Ca} channel blocker. The voltage pulses applied are shown below current traces of the control (mock). (B) Current density–voltage relationships of 1 μM Pax sensitive currents in three groups are shown. (C) Current density of 1 μM Pax sensitive currents at 120 mV is compared between three groups. $^{*}p < 0.05$; $^{**}p < 0.01$ vs. mock.

KCa1.1-mCherry/GFP (mock, 364 ± 60 pA/pF, $n = 5$, $p < 0.01$; Fig. 1B and C).

It has been reported that over expression of cav1 inhibits BK_{Ca} channel expression on plasma membrane in HEK293 cells [17] and bovine aortic endothelial cells [16]. These results suggest that co-expression of cav3 (and cav1 as well) shows inhibitory effect on functional expression of BK_{Ca} channels in HEK293 cells. Although the reason of these results are unknown, it has been reported that co-expression of cav1 reduces the number of BK_{Ca} channels reaching the cell surface by 60–70% but does not modify electric properties of the channels [17]. In human myometrium, unfused caveolae containing BK_{Ca} channels were observed beneath the cell surface [20]. It is possible the over expression of cav1/cav3 may increase the number of unfused caveolae and BK_{Ca} channels included in them.

3.2. Caveolin-3 was co-localized with BK_{Ca} channel in plasma membrane via direct interaction

In the next series of experiments, we examined localization of BK_{Ca} channel and cav3 on plasma membrane using TIRF microscope in HEK293 cells, which were transfected with KCa1.1-mCherry and GFP-cav3 cDNAs. KCa1.1-mCherry alone, GFP-cav3 alone and co-localized KCa1.1-mCherry/GFP-cav3 were detected as red, green and yellow dots, respectively, in TIRF images (Fig. 2Aa and Online Movie I). The co-localization of KCa1.1-mCherry/GFP-cav3 was not incident, since each set of red (KCa1.1-mCherry) and green (GFP-cav3) particles merged as a yellow dot in all sequential images taken every second for over 60 s (see the trajectories of particles a–c indicated as inset of TIRF images in Fig. 2A). It is noteworthy that the relative fluorescence intensity of KCa1.1-mCherry co-localized with GFP-cav3 (3.0 ± 0.7, $n = 16$) was significantly larger than that of KCa1.1-mCherry alone (1.0 ± 0.3, $n = 31$, $p < 0.05$) (Fig. 2Aa). Correspondingly, in cells co-expressing KCa1.1-mCherry and GFP-cav1, the signals from KCa1.1-mCherry alone, GFP-cav1 alone and KCa1.1-mCherry/GFP-cav1 co-localization were detected as shown in the previous study [19]. The relative fluorescence intensity of KCa1.1-mCherry co-localized with GFP-cav1 (3.5 ± 1.1, $n = 13$) was significantly larger than that of KCa1.1-mCherry alone (1.0 ± 0.2, $n = 24$, $p < 0.05$) (Fig. 2Ab and Online Movie II).

To obtain a line of precise evidence indicating the direct molecular interaction between BK_{Ca} channel (BKα) with cav3, FRET analyses with acceptor photobleaching method using CFP (donor) and YFP (acceptor) pair were performed. The ratio of co-localization was 40.3 ± 8.4% ($n = 19$) in cells co-expressing KCa1.1-YFP and CFP-cav3, and 56.6 ± 10.5% ($n = 6$) in cells co-expressing KCa1.1-YFP and CFP-cav1 (Fig. 2C). After KCa1.1-YFP bleaching, the increase of fluorescence intensity from CFP was observed both in CFP-cav3 (Fig. 2Ba) and CFP-cav1 (Fig. 2Bb) in these co-localized particles. HEK293 cells expressing CFP-cav3 alone were used as negative control. The E_{FRET} was 4.3 ± 0.9% ($n = 19$), 6.9 ± 1.1% ($n = 6$) and −2.4 ± 1.4% ($n = 11$) in cells expressing KCa1.1-YFP/CFP-cav3, KCa1.1-YFP/CFP-cav1 and CFP-cav3 alone, respectively ($p < 0.01$ vs. CFP-cav3 alone, Fig. 2D).

In addition, to confirm the direct molecular interaction between BK_{Ca} channel and cav3, we also used the conventional co-immunoprecipitation methods. The results indicate that GFP-cav3 as well as GFP-cav1 directly binds to FLAG-KCa1.1 (Supplemental Fig. 1A). Taken together, it can be concluded that cav3 molecule directly interacts with BK_{Ca} channels as protein–protein interaction and acts together in living cells. It has been reported that cav1 monomers assemble into multivalent oligomers containing 14–16 monomers [21] or 7 monomers [22] per oligomer. Cav3 has been also reported to form a disc-shaped nonamer [23]. These individual caveolin oligomers can interact with each other to form caveola structures. The fluorescence intensity of GFP-cav3 or GFP-cav1 co-localized with KCa1.1-mCherry was significantly larger than that of GFP-cav3 or GFP-cav1 alone (data not shown), as shown in a similar manner for the intensity of KCa1.1-mCherry in Fig. 2A. These results from TIRF imaging strongly suggest that BK_{Ca} channels are accumulated as molecular complex with cav3 or cav1 homo-oligomers and maybe also with cav1/3 hetero-oligomers as well [24]. Further quantitative analyses were, however, remains to be determined.

3.3. Caveolin-3 interacted with BK_{Ca} channel via caveolin-1 binding motif

Finally we investigated the region of BK_{Ca} channel responsible for the direct interaction with cav3. Cav1 binding motif is thought to be ΦXΦXXXXΦ and ΦXXXXXΦXXΦ, where Φ is an aromatic amino acid and X is any amino acid [25]. BK_{Ca} channel has a cav1 binding motif (^{1072}YNMLCFGIY^{1080}) within its C terminus [17]. It has been shown that BKα-subunit mutant, which lacks the cav1 binding motif, cannot be expressed on cell surface in HEK293 cells [17]. We deleted this cav1 binding motif from KCa1.1-YFP (KCa1.1ΔCB-YFP) and examined FRET interaction using TIRF microscope. As shown in Fig. 3A, KCa1.1ΔCB-YFP did not form dot-like signal as in Fig. 2A and B, and supposed to be localized mainly in cytosol. On the other hand, co-expressed GFP-cav3 or GFP-cav1 was observed in plasma membrane and showed dot-like fluorescence signals. FRET interaction between KCa1.1ΔCB-YFP and CFP-cav3 (1.5 ± 0.6%, $n = 14$) was markedly attenuated than that between KCa1.1-YFP and CFP-cav3 (4.4 ± 1.1%, $n = 14$, $p < 0.05$, Fig. 3Ba). Similarly, CFP-cav1 showed decreased FRET efficiency (0.8 ± 0.8% with KCa1.1ΔCB-YFP, $n = 22$, vs. 6.2 ± 1.1% with KCa1.1-YFP, $n = 5$, $p < 0.01$, Fig. 3Bb). These results strongly suggest

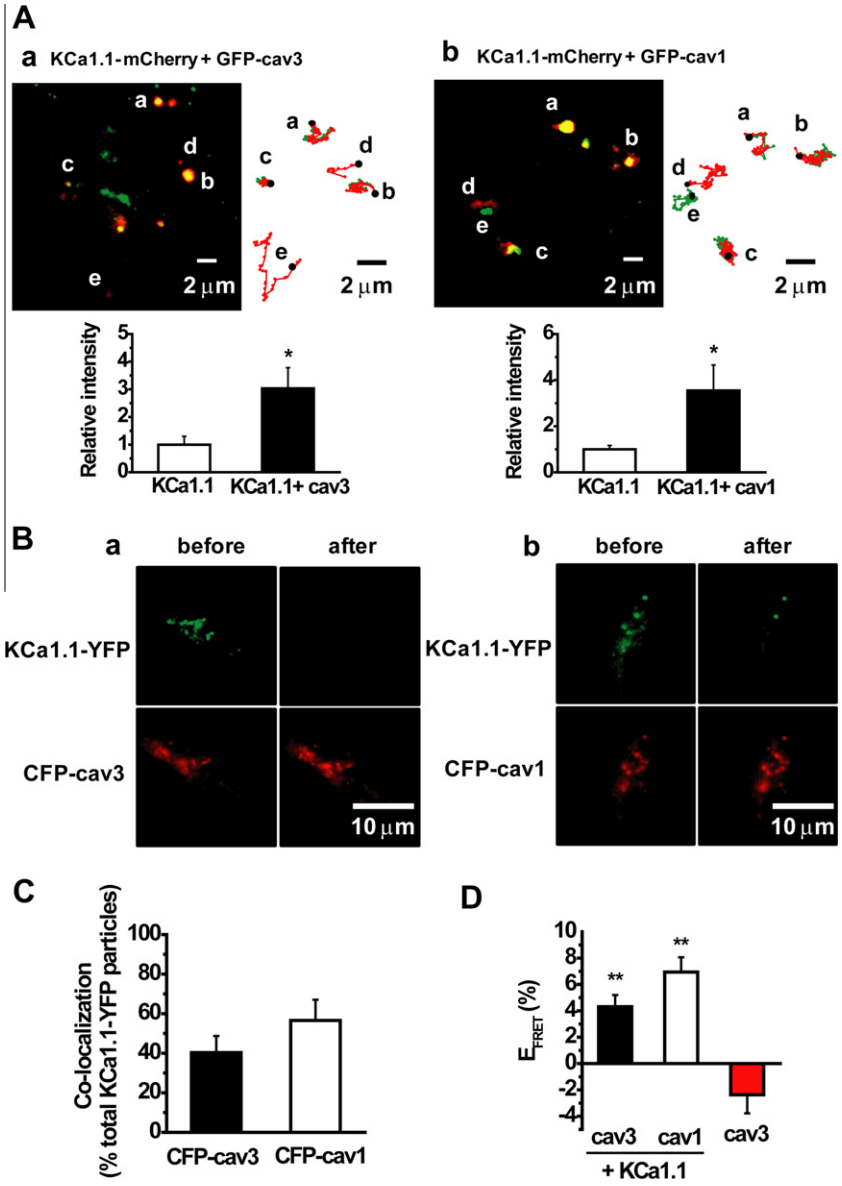

Fig. 2. (A) TIRF images of HEK293 cells co-expressing KCa1.1-mCherry and GFP-cav3 (Aa), or KCa1.1-mCherry and GFP-cav1 (Ab) are shown. mCherry and GFP fluorescence are indicated by red and green signals, respectively (Online Movie I and II). The fluorescent particles of KCa1.1-mCherry and GFP-cav3 molecules on the cell surface were indicated as particles a–e in the image "A". The signals were tracked for 60 s and shown in insets, respectively. Note that KCa1.1-mCherry and GFP-cav3 molecules move together during the measurements (a–c). Black dots indicate starting points of tracking. The relative fluorescence intensity of KCa1.1-mCherry co-localized with cav3 or cav1 are shown below. $^{*}p < 0.05$ vs. KCa1.1. (B) TIRF images of HEK293 cells co-expressing KCa1.1-YFP and CFP-cav3 (a), or KCa1.1-YFP and CFP-cav1 (b) were taken before and after KCa1.1-YFP bleaching. CFP and YFP fluorescence are indicated by red and green signals, respectively. The increase in CFP fluorescence was detected in both CFP-cav3 expressing and CFP-cav1 expressing cells. (C) The ratio of co-localization against total KCa1.1-YFP particles was measured in CFP-cav3 expressing cells (CFP-cav3) or CFP-cav1 expressing cells (CFP-cav1). (D) FRET efficiency (E_{FRET}) was compared between three groups. HEK293 cells expressing CFP-cav3 alone were used as negative control. $^{**}p < 0.01$ vs. cav3.

that cav3 molecule interacts with KCa1.1 at the same site as cav1 does. In addition, it is confirmed that ^{1072}YNMLCFGIY^{1080} is essential domain for the expression of KCa1.1 to cell surface, in addition for the binding to cav1 and cav3 [17].

The lack of direct molecular interaction between KCa1.1ΔCB and cav3 in cell free system was also examined by use of the conventional co-immunoprecipitation methods. The results indicate that neither GFP-cav3 nor GFP-cav1 binds to FLAG-KCa1.1ΔCB (Supplemental Fig. 1B).

The functional interaction between cav3 and BK_{Ca} channel is most likely in skeletal muscles. Within the sarcolemma, cav3 binds to β-dystroglycan and forms the dystrophin complex to confer stability to sarcolemma [15]. Loss of cav3 [26] or dominant-negative cav3 mutants [27] induces the defects in the dystrophin complex and leads to skeletal muscular disease, such as LGMD-1C. Conversely cav3 transgenic mice, which over-express wild-type cav3, show Duchenne-like muscular dystrophy phenotype caused by down-regulation of dystrophin and β-dystroglycan protein expression [28]. The dystrophin complex not only forms skeletal muscle structures but also functions as signal domains by accumulating several signal molecules, such as neuronal nitric oxide synthase, calmodulin-dependent protein kinase II, protein kinase A, etc. [29]. It has been suggested that, in skeletal muscle from *C. elegans*, BK_{Ca} channel expresses and functions stably by coupling with auxiliary subunits (BKIP [6], ISLO-1 [7]), a cytoskeletal protein (α-catulin [8,9]) and the dystrophin complex [11] and its components

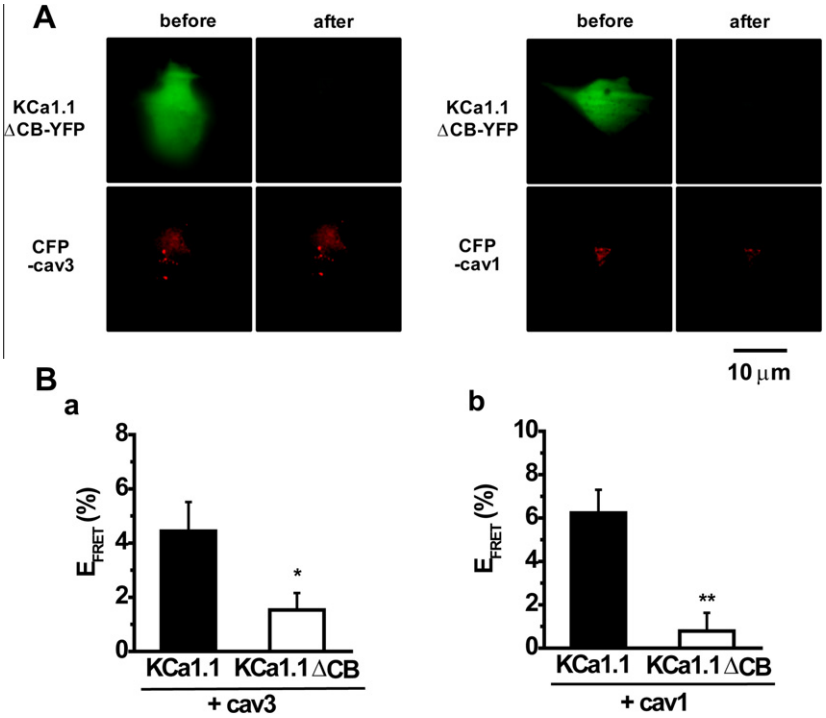

Fig. 3. (A) TIRF images of HEK293 cells co-expressing KCa1.1ΔCB-YFP and CFP-cav3 (left), and KCa1.1ΔCB-YFP and CFP-cav1 (right) were obtained before and after KCa1.1ΔCB-YFP bleaching shown. (Ba) FRET efficiency (E_{FRET}) in cells co-expressing KCa1.1-YFP and CFP-cav3 or KCa1.1ΔCB-YFP and CFP-cav3 was compared. $^{*}p < 0.05$ vs. KCa1.1. (Bb) FRET efficiency (E_{FRET}) in cells co-expressing KCa1.1-YFP and CFP-cav1, and KCa1.1ΔCB-YFP and CFP-cav1 was compared. $^{**}p < 0.01$ vs. KCa1.1.

(DYS-1 [10], dystrobrevin [5]). In addition to forming the dystrophin complex, cav3 also functions as signal domains [30] and interacts with voltage-dependent Ca^{2+} channel [31] and ryanodine receptor 1 (RyR1) [23,32], and contributes to excitation–contraction coupling (E–C coupling) [33]. Cav3 scaffolding domain (^{55}DGVWKVSYTTFTVSKYWCYR^{74}) is 75% identical to cav1 scaffolding domain (^{82}DGIWKASFTTFTVTKYWFYR^{101}) [12], and, as shown in Fig. 3, cav3 directly binds to cav1 binding domain in BKα (^{1072}YNMLCFGIY^{1080}). These findings, including our present results, strongly support the assumption that cav3 molecule directly interacts with BK_{Ca} channels to keep in the functional dystrophin molecular complex of caveolin-associated signal domains and stabilizes its surface expression. Cav3 may also accumulate other signal molecules into the dystrophin complex and modulates BK_{Ca} channels functions.

In conclusion, cav3 possesses direct interaction with KCa1.1, at the same domain for cav1 binding, to regulate the trafficking to cell surface and also to form functional molecular complex in living reconstituted system of HEK293 cells.

Acknowledgments

This investigation was supported by a Grant-in-Aid for Scientific Research on Priority Areas (20056027; to Y.I.) from the Ministry of Education, Culture, Sports, Science, and Technology, and Grant-in-Aids for Scientific Research (B) (23390020; to Y.I.), and Grant-in-Aid for JSPS Fellows (22-6641; to Y.S.) from the Japan Society for the Promotion of Science.

Appendix A. Supplementary data

Supplementary data associated with this article can be found, in the online version, at http://dx.doi.org/10.1016/j.bbrc.2012.12.015.

References

[1] J. Cui, H. Yang, U.S. Lee, Molecular mechanisms of BK channel activation, Cell Mol. Life Sci. 66 (2009) 852–875.
[2] S. Ghatta, D. Nimmagadda, X. Xu, S.T. O'Rourke, Large-conductance, calcium-activated potassium channels: structural and functional implications, Pharmacol. Ther. 110 (2006) 103–116.
[3] R. Latorre, C. Vergara, C. Hidalgo, Reconstitution in planar lipid bilayers of a Ca^{2+}-dependent K^+ channel from transverse tubule membranes isolated from rabbit skeletal muscle, Proc. Natl. Acad. Sci. USA 79 (1982) 805–809.
[4] H.G. Knaus, A. Eberhart, R.O. Koch, P. Munujos, W.A. Schmalhofer, J.W. Warmke, G.J. Kaczorowski, M.L. Garcia, Characterization of tissue-expressed alpha subunits of the high conductance Ca^{2+}-activated K^+ channel, J. Biol. Chem. 270 (1995) 22434–22439.
[5] B. Chen, P. Liu, H. Zhan, Z.W. Wang, Dystrobrevin controls neurotransmitter release and muscle Ca^{2+} transients by localizing BK channels in *Caenorhabditis elegans*, J. Neurosci. 31 (2011) 17338–17347.
[6] B. Chen, Q. Ge, X.M. Xia, P. Liu, S.J. Wang, H. Zhan, B.A. Eipper, Z.W. Wang, A novel auxiliary subunit critical to BK channel function in *Caenorhabditis elegans*, J. Neurosci. 30 (2010) 16651–16661.
[7] H. Kim, J.T. Pierce-Shimomura, H.J. Oh, B.E. Johnson, M.B. Goodman, S.L. McIntire, The dystrophin complex controls BK channel localization and muscle activity in *Caenorhabditis elegans*, PLoS Genet. 5 (2009) e1000780.
[8] L.S. Abraham, H.J. Oh, F. Sancar, J.E. Richmond, H. Kim, An alpha-catulin homologue controls neuromuscular function through localization of the dystrophin complex and BK channels in *Caenorhabditis elegans*, PLoS Genet. 6 (2010).
[9] B. Chen, P. Liu, S.J. Wang, Q. Ge, H. Zhan, W.A. Mohler, Z.W. Wang, α-catulin CTN-1 is required for BK channel subcellular localization in *C. elegans* body-wall muscle cells, EMBO J. 29 (2010) 3184–3195.
[10] M. Carre-Pierrat, K. Grisoni, K. Gieseler, M.C. Mariol, E. Martin, M. Jospin, B. Allard, L. Segalat, The SLO-1 BK channel of *Caenorhabditis elegans* is critical for muscle function and is involved in dystrophin-dependent muscle dystrophy, J. Mol. Biol. 358 (2006) 387–395.
[11] F. Sancar, D. Touroutine, S. Gao, H.J. Oh, M. Gendrel, J.L. Bessereau, H. Kim, M. Zhen, J.E. Richmond, The dystrophin-associated protein complex maintains muscle excitability by regulating Ca^{2+}-dependent K^+ (BK) channel localization, J. Biol. Chem. 286 (2011) 33501–33510.
[12] B. Razani, S.E. Woodman, M.P. Lisanti, Caveolae: from cell biology to animal physiology, Pharmacol. Rev. 54 (2002) 431–467.
[13] A.W. Cohen, R. Hnasko, W. Schubert, M.P. Lisanti, Role of caveolae and caveolins in health and disease, Physiol. Rev. 84 (2004) 1341–1379.
[14] H.H. Patel, F. Murray, P.A. Insel, Caveolae as organizers of pharmacologically relevant signal transduction molecules, Annu. Rev. Pharmacol. Toxicol. 48 (2008) 359–391.

[15] E. Gazzerro, F. Sotgia, C. Bruno, M.P. Lisanti, C. Minetti, Caveolinopathies: from the biology of caveolin-3 to human diseases, Eur. J. Hum. Genet. 18 (2010) 137–145.
[16] X.L. Wang, D. Ye, T.E. Peterson, S. Cao, V.H. Shah, Z.S. Katusic, G.C. Sieck, H.C. Lee, Caveolae targeting and regulation of large conductance Ca^{2+}-activated K^+ channels in vascular endothelial cells, J. Biol. Chem. 280 (2005) 11656–11664.
[17] A. Alioua, R. Lu, Y. Kumar, M. Eghbali, P. Kundu, L. Toro, E. Stefani, Slo1 caveolin-binding motif, a mechanism of caveolin-1-Slo1 interaction regulating Slo1 surface expression, J. Biol. Chem. 283 (2008) 4808–4817.
[18] R. Lu, A. Alioua, Y. Kumar, M. Eghbali, E. Stefani, L. Toro, MaxiK channel partners: physiological impact, J. Physiol. 570 (2006) 65–72.
[19] H. Yamamura, C. Ikeda, Y. Suzuki, S. Ohya, Y. Imaizumi, Molecular assembly and dynamics of fluorescent protein-tagged single KCa1.1 channel in expression system and vascular smooth muscle cells, Am. J. Physiol. Cell Physiol. 302 (2012) C1257–C1268.
[20] A.M. Brainard, A.J. Miller, J.R. Martens, S.K. England, Maxi-K channels localize to caveolae in human myometrium: a role for an actin-channel-caveolin complex in the regulation of myometrial smooth muscle K^+ current, Am. J. Physiol. Cell Physiol. 289 (2005) C49–C57.
[21] M. Sargiacomo, P.E. Scherer, Z. Tang, E. Kubler, K.S. Song, M.C. Sanders, M.P. Lisanti, Oligomeric structure of caveolin: implications for caveolae membrane organization, Proc. Natl. Acad. Sci. USA 92 (1995) 9407–9411.
[22] I. Fernandez, Y. Ying, J. Albanesi, R.G. Anderson, Mechanism of caveolin filament assembly, Proc. Natl. Acad. Sci. USA 99 (2002) 11193–11198.
[23] G. Whiteley, R.F. Collins, A. Kitmitto, Characterization of the molecular architecture of human caveolin-3 and interaction with the skeletal muscle ryanodine receptor, J. Biol. Chem. 287 (2012) 40302–40316.
[24] F. Capozza, A.W. Cohen, M.W. Cheung, F. Sotgia, W. Schubert, M. Battista, H. Lee, P.G. Frank, M.P. Lisanti, Muscle-specific interaction of caveolin isoforms: differential complex formation between caveolins in fibroblastic vs. muscle cells, Am. J. Physiol. Cell Physiol. 288 (2005) C677–C691.
[25] J. Couet, S. Li, T. Okamoto, T. Ikezu, M.P. Lisanti, Identification of peptide and protein ligands for the caveolin-scaffolding domain. Implications for the interaction of caveolin with caveolae-associated proteins, J. Biol. Chem. 272 (1997) 6525–6533.
[26] F. Galbiati, J.A. Engelman, D. Volonte, X.L. Zhang, C. Minetti, M. Li, H. Hou Jr., B. Kneitz, W. Edelmann, M.P. Lisanti, Caveolin-3 null mice show a loss of caveolae, changes in the microdomain distribution of the dystrophin–glycoprotein complex, and t-tubule abnormalities, J. Biol. Chem. 276 (2001) 21425–21433.
[27] Y. Sunada, H. Ohi, A. Hase, T. Hosono, S. Arata, S. Higuchi, K. Matsumura, T. Shimizu, Transgenic mice expressing mutant caveolin-3 show severe myopathy associated with increased nNOS activity, Hum. Mol. Genet. 10 (2001) 173–178.
[28] F. Galbiati, D. Volonte, J.B. Chu, M. Li, S.W. Fine, M. Fu, J. Bermudez, M. Pedemonte, K.M. Weidenheim, R.G. Pestell, C. Minetti, M.P. Lisanti, Transgenic overexpression of caveolin-3 in skeletal muscle fibers induces a Duchenne-like muscular dystrophy phenotype, Proc. Natl. Acad. Sci. USA 97 (2000) 9689–9694.
[29] G.S. Pilgram, S. Potikanond, R.A. Baines, L.G. Fradkin, J.N. Noordermeer, The roles of the dystrophin-associated glycoprotein complex at the synapse, Mol. Neurobiol. 41 (2010) 1–21.
[30] R.C. Balijepalli, T.J. Kamp, Caveolae, ion channels and cardiac arrhythmias, Prog. Biophys. Mol. Biol. 98 (2008) 149–160.
[31] H. Couchoux, B. Allard, C. Legrand, V. Jacquemond, C. Berthier, Loss of caveolin-3 induced by the dystrophy-associated P104L mutation impairs L-type calcium channel function in mouse skeletal muscle cells, J. Physiol. 580 (2007) 745–754.
[32] S. Vassilopoulos, S. Oddoux, S. Groh, M. Cacheux, J. Faure, J. Brocard, K.P. Campbell, I. Marty, Caveolin 3 is associated with the calcium release complex and is modified via in vivo triadin modification, Biochemistry 49 (2010) 6130–6135.
[33] N.D. Ullrich, D. Fischer, C. Kornblum, M.C. Walter, E. Niggli, F. Zorzato, S. Treves, Alterations of excitation–contraction coupling and excitation coupled Ca^{2+} entry in human myotubes carrying CAV3 mutations linked to rippling muscle, Hum. Mutat. 32 (2011) 309–317.